Drier Mediterranean Soils due to Greenhouse Warming bring easterly Winds over Summertime Central Europe

Reindert J. Haarsma, Frank Selten, Bart vd Hurk,

Wilco Hazeleger and Xueli Wang

Royal Netherlands Meteorological Institute (KNMI)

De Bilt, The Netherlands

Abstract

Western European summers become more continental in simulations for the 21st century. Anomalously large summer warming over the Mediterranean area in concert with drier soils and a reduced surface pressure can explain this change. The warming is enhanced due to soil moisture depletion which limits the cooling of the land surface by evaporation. A large-scale Mediterranean heat low develops, bringing easterly winds over Central Europe. Statistical analysis for present-day conditions indicates that the same mechanism operates on intra-seasonal timescales; dry Mediterranean soils in June are correlated with high temperature and low surface pressure in July-August. Idealized simulations confirm the relation between the surface warming of the Mediterranean area and the development of a heat low. The development of a heat low in response to dry soils induces a positive feedback: drier Mediterranean soils in summer bring easterly winds over Europe and increase the continental character of Western European summer climate.

Introduction

Many studies on the impact of greenhouse warming on European summer conditions have focused on the heat budget and the hydrological cycle. Most of these [e.g. Sterl et al. 2008, Stott et al. 2004, Schär et al. 2004, Fischer et al. 2007] point towards a hotter and more arid climate with a larger number of long lasting heat waves due to a positive feedback between drier soils and surface air temperatures (SAT). Changes in atmospheric circulation have received less attention. The multi-model response of CMIP3 [Meehl et al, 2007] as discussed in the Fourth Assessment Report (AR4) of the IPCC (2007) and shown in Fig. 10.9 therein, however, displays a significant decrease of mean sea level pressure (MSLP) over North Africa and the Mediterranean area. Consistent with this an increase of easterly winds over Central Europe is found in most of the CMIP3 simulations [Van Ulden and Oldenborgh, 2006]. These easterly winds enhance the warming and drying over Central Europe. Using statistical analyses and additional climate model simulations we demonstrate that the decrease of MSLP can be understood as a large-scale heat low response to the drying and enhanced warming of that area.

Models

For the analysis of the change in the summer circulation over Europe we have used the output of two climate models: the ECHAM5/OMI model used in the ensemble experiment ESSENCE [Sterl et al. 2008] and the integrated forecasting system (IFS) atmosphere model of the European Centre of Medium Range Weather Forecast (ECMWF) cycle 31R1. The ECMWF model is the atmospheric component of the earth system model EC-EARTH that is under development in a joint project of several European institutes. Both models simulate rather well the climate over Europe. The large ensemble of ESSENCE ensures statistical robustness whereas the flexibility of the ECMWF model enables sensitivity experiments.

ESSENCE

In ESSENCE seventeen model integrations between 1950 and 2100 were carried out at a resolution of T63L31 using slightly perturbed initial atmospheric conditions. For 1950-2000 the concentrations of greenhouse gases (GHG) and tropospheric sulfate aerosols are specified from observations, while for 2001-2100 they follow the SRES A1b scenario. Stratospheric aerosols from volcanic eruptions are not taken into account and the solar constant is fixed. The runs are initialized from a long run in which historical GHG concentrations have been used until 1950 [Sterl et al. 2008]. The data was analyzed for 1971-2000 and 2071-2100 which will be denoted henceforth as present and future.

ECMWF

The ECMWF model was run at resolution T95L40. Time slice experiments were made for the present (1971-2000) and future (2071-2100) climate. These experiments consisted of ensembles of 5 runs of 10 year duration starting from different atmospheric initial conditions. In the analysis the first year was neglected, resulting in 45 years of data for each period. For the present climate observed climatological sea surface temperatures (SST), sea-ice, tropospheric sulfate aerosols and GHG concentrations were prescribed. Future aerosols and GHG's were derived from the SRES A1b scenario. Future SST and sea-ice coverage corresponded to the multi-model ensemble mean seasonal cycle of 2071-2100 of selected CMIP3 SRES A1b climate scenario simulations (ECHAM5/OMI, GFDL-CM2.1, UKMO-HADGEM1 and MIROC3.2 (hires)). For details on these model simulations see table 8.1, 10.1 and 10.4 of AR4.

Results

Changes in summer circulation caused by greenhouse warming

Figure 1, panels a and b displays the ensemble mean change in MSLP during June-August (JJA) for ESSENCE and ECMWF. Both models simulate increased surface pressure over the British Isles and lower pressure over Southern Europe and the Mediterranean area. This change in the pressure distribution is similar to the CMIP3 multi-model response displayed in AR4 (Fig. 10.9) and induces an increased easterly flow over Central Europe. This is clearly seen in Fig. 1, panels g and h, showing an increase of days with easterly flow .

The vertical structure of the height field (Fig. 1, panels e and f), zonally averaged over the European sector, shows that the low has its maximum at the surface and extends to about 800 hPa, whereas the high over the British Isles extends vertically over the entire troposphere with a tilt towards the south. These results suggests that the Mediterranean low is not the result of a change in the planetary wave structure, which we would expect to be equivalent barotropic, but due to a change in surface forcing.

Both models simulate a relatively large increase in land SAT in the Mediterranean area (Fig. 1, panels c and d). Compared to Northern Europe and the Atlantic the relative increase in SAT is about 3 °C. These diagnostics suggest that the low pressure response over the Mediterranean area can be understood as a heat low response to the enhanced warming. In an earlier study addressing the Sahel rainfall Haarsma et al. [2005] demonstrated that enhanced heating of Northern Africa leads to a heat low response over the Sahara.

The enhanced warming over the Mediterranean area is confined to the land areas. Above sea the surface warming is moderate, but above 925 hPa (not shown) a rather uniform enhanced warming over the entire Mediterranean area is simulated. This uniform warming is caused by the advection of warm land air masses to the sea, partly by the land-sea breezes and by the adiabatic warming due to subsidence over the sea. The warming is confined to the lower troposphere. We therefore expect that a heat low mechanism operates for the entire Mediterranean area notwithstanding the relatively cool Mediterranean Sea.

Intraseasonal time scales

We first tested the Mediterranean heat low hypothesis and its relation to dry soils on intra-seasonal time scales using monthly mean ESSENCE data. A lagged Singular Value Decomposition (SVD) analysis is applied, which is designed to find spatial patterns of (lagged) fields with a maximum covariation [Bretherton et al. 1992]. To indicate the soilwetness we use WS = $(\omega-\omega_{pwp})/(\omega_{cap}-\omega_{pwp})$, where ω is the average moisture content of the upper meter of the soil, ω_{cap} the volumetric water content at field capacity and ω_{pwp} at wilting point [van den Hurk et al. 2000]. A weak but statistically significant relationship is detected in the Mediterranean area between WS in June and MSLP in July-August (JA) (Fig. 2, panels a and b). This implies that anomalously low Mediterranean soil moisture in June increases the likelihood of low pressures during July-August. Due to the large data set of ESSENCE (850 summer seasons) this relationship is statistically significant. For individual members, with 30 summer seasons, it is not.

A regression analysis of the amplitude of the dominant SVD WS pattern in June with evaporation (Fig. 2c) and SAT (Fig. 2d) in JA reveals anomalously high temperatures in the dry areas with a reduced latent heat flux, confirming that the low pressure anomaly pattern in JA has indeed the characteristics of a heat low. The correlations are statistically significant but small (0.4 at maximum) which implies that WS in June explains only a small fraction of the variance in SAT and MSLP in July-August (about 20%). The latent heat flux in JA is reduced due to drier soils (not shown).

Soils in JA are drier due to persistence and less rainfall (Fig. 2e) indicating a positive feedback. The largest signal in rainfall, however, is not seen over the areas with the largest reduction in evaporation, but over central and eastern Europe where the largest gradient in MSLP is located (Fig. 2b). This suggests that there the rainfall reduction is mainly due to the enhanced easterly winds that block the inflow of moist maritime air from the Atlantic.

Vautard et al. [2007] noted a northward propagation of dry conditions during hot summers and explained this by the northward transport of anomalously warm and dry air from Southern Europe during southerly wind episodes. By comparing the change in precipitation found during predominantly northerly and southerly wind conditions we confirmed his results for ESSENCE and ECMWF (not shown). Our results indicate, moreover, that the heat low response, blocking the inflow of moist maritime air is an additional mechanism for the northward expansion of dry conditions. Vautard et al [2007] also noted that hot summers tend to be preceded by winter rainfall deficits over Southern Europe. Also the ESSENCE data indicate that dry soil conditions in June tend to be preceded by low rainfall amounts in January-May (Fig. 2f).

Mediterranean heating experiment

To check whether enhanced heating of the Mediterranean area generates lower pressures similar to observed in the simulations for the future climate, we performed additional simulations with the ECMWF model. For the present climate we artificially increased SAT by adding 35 W m^{-2} to the net downward surface flux over the Mediterranean region (25-45º N, 10º W - 40º E), with a linear decrease to 0 Wm^{-2} between 30-25° N and 45-50° N (MEDFLUX experiment).

The simulated increase in SAT during summer is 2-3 ºC (Fig. 3a), similar to the ECMWF and ESSENCE climate change results (Fig. 1, panels a and b). In response to this lower tropospheric warming a Mediterranean heat low of about 1-1.5 hPa develops (Fig. 3b), resulting in an increase of days with easterly winds over Central Europe (Fig. 3c). The increase is less than in Fig. 1g because of the absence of the high above the British Isles. The heat low is connected to rising air and a baroclinic response in the upper troposphere, similar as noted by Fisher et al. [2007]. The anomalous upper air divergence that accompanies the anomalous rising motion generates a Rossby wave train with an equivalent barotropic response. The structure of this wave train over Europe is seen in Fig. 3c north of 50° N. Although this response has some similarities with the climate change response (Fig. 1e) it is substantially different. This is because the structure of this wave train is also affected by other remote causes like for instance the change in tropical SST.

Causes of enhanced SAT over the Mediterranean area in the greenhouse warming experiments

The relatively large increase of SAT over the Mediterranean area is related to the depletion of soil moisture resulting in a strong decrease in latent heat flux. The decrease in latent heat flux, especially along the north coast of the Mediterranean sea, is clearly seen in Fig. 4a. It seems large enough (10-20 W m^{-2}) to explain the relative SAT increase . The change in surface solar radiation is small in this area (Fig. 4e). The drying is not confined to the Mediterranean area; in fact Fig. 4b shows that the largest drying occurs in western and central Europe. The drying, however, most strongly reduces the latent heat flux and increases the SAT in the Mediterranean area because of the semi-arid conditions with low WS values of about of 0.2. A further reduction of WS in this region has a large impact on evaporation due to the non-linear dependence of evaporation on WS.

Over central Europe there is a widespread increase in subsidence (Fig. 4d) resulting in a reduction of cloud cover, precipitation (Fig. 4c) and an increase of surface solar radiation (Fig. 4e). Here the solar radiation increase is an important warming term in the surface heat balance that is partly offset by an increased latent heat flux. Over the Mediterranean area the development of a heat low decreases the subsidence, but it remains an area dominated by large-scale subsidence with clear skies and little precipitation.

Causes of drier European soils

Both increasing evaporation and decreasing precipitation cause local drying of the soil. The rate of evaporation is proportional to the vertical gradient of specific humidity at the surface. In a warming world this gradient increases, when all else stays the same, due to the nonlinearity of the Clausius Clapeyron relation. So, as long as soil moisture is available, a stronger evaporation can be expected, contributing to the drying of the soil. In regions of low relative humidity and subsidence like the Mediterranean area this enhanced evaporation is not compensated by increased rainfall. In central Europe the drying is enhanced by the increased subsidence resulting in a reduction of rainfall (Fig. 4c).

The increased subsidence over Europe is the result of the north-eastward extension of the climatological subtropical anticyclone over the Atlantic. This appears to be related to the widening of the Hadley circulation [Seager et al. 2007] and to the subsequent northward shift of the storm tracks especially over the eastern part of the Atlantic and Europe. For the winter season this is documented for the ESSENCE model by Pinto et al. [2007]. A similar shift is also simulated by the ECMWF model (not shown). The northward shift of the storm tracks in March-May results in a reduction of the rainfall in the western Mediterranean area (Fig. 4f). The results of ESSENCE (Fig. 2) demonstrated that on seasonal time scales reduced winter-spring rainfall results in enhanced summer drying. Similarly reduced winter-spring rainfall caused by greenhouse warming also increases the summer drying.

Discussion

Using the ESSENCE data set a relationship has been detected between the depletion of soil moisture in early summer and the development of a heat low over the Mediterranean area in late summer. The projected climate change in summertime Europe due to global warming is shaped by this mechanism of internal variability and explains the increased easterlies in Central Europe at the northern flank of this heat low.

A rather robust result of the CMIP3 climate simulations is an enhanced warming of the Mediterranean area in JJA (See Fig. 11.5 of AR4). This enhanced warming generates an anomalous heat low as verified in an idealized experiment in which the Mediterranean area is artificially heated in the present climate. The resulting increase of SAT and pressure reduction over the Mediterranean area is comparable to that simulated by the ECMWF and ESSENCE model for the end of this century under the SRES A1b scenario and the multi-model climate change of CMIP3 (See Fig. 10.9 of AR4)

The connection between drier soils and higher SAT in response to greenhouse warming appears to be a robust mechanism [Vautard et al. 2007, Rowell and Jones 2006]. In addition, the development of a heat low at the surface in response to drier soils and higher SAT is also confirmed in various studies [Ferranti and Viterbo 2006, Fischer et al 2007]. Here we show that the combination of these two mechanisms results in the development of a heat low over the Mediterranean area that appears to be the dominant climate response in MSLP over that region. Our results are consistent with Hoinka et al. [2007] who noted an intensification of the Iberian heat low in response to greenhouse warming.

Acknowledgements

We thank the DEISA Consortium (www.deisa.eu), co-funded through EU FP6 projects RI-508830 and RI-031513, for support within the DEISA Extreme Computing Initiative.

References

Bretherton, C.S., C. Smith and J.M. Wallace (1992), An intercomparison of methods for finding coupled patterns in climate data. *J. Climate, 5,* 541-560.

Ferranti, L. and P. Viterbo (2006), The European summer of 2003: Sensitivity to soil water initial conditions. *J. Clim., 19,* 3659-3680.

Fischer, E.M., S.I. Seneviratne, P.I. Vidale, D. Lüthi and C. Schär (2007), Soil moisture-atmosphere interactions during the 2003 European summer heat wave. *J. Clim., 20,* 5081-5099.

Haarsma, R.J., F.M. Selten, S.L. Weber and M. Kliphuis (2005), Sahel rainfall variability and response to greenhouse warming. *Geophys. Res. Lett., 32,* doi:10.1029/2005GL023232.

Hoinka, K.P., M. Gaertner and M. de Castro (2007) Iberian thermal lows in a changed climate. *Quart. J. Royal Met. Soc., 133,* 1113-1126, doi:10.1002/qj.78.

IPCC (2007), Climate Change 2007, The Physical Science Basis. *Contribution of Working Group I to the Fourth Assessment Report on the Intergovernamental Panel on Climate Change,*[Solomon, S., D. Qin, M. Manning, Z. Chen, M. Marquis, K. B. Averyt, M. Tignor and H.L. Miller (eds)] Cambridge University Press, Cambridge, United Kingdom and New York, USA, 996 pp.

Meehl, G.A., C. Covey, T. Delworth, M. Latif, B. McAvaney, J.F.B. Mitchell, R.J. Stouffer and K.E. Taylor (2007), The WCRP CMIP3 multi-model dataset. *Bull. Amer. Meteor. Soc., 88,* 1383-1394, doi:10.1175/BAMS-88-9-1383.

Pinto, J.G, U. Ulbrich, G.C. Leckebusch, T. Spangehl, M. Reyers and S. Zacharias (2007), Changes in storm track and cyclone activity in three SRES ensemble experiments with the ECHAM5/MPI-OM1 GCM. *Clim. Dyn., 29,* 195-210. doi:10.1007/s00382-007-0230-4

Rowell, D.P. and R.G. Jones (2006), Causes and uncertainty of future summer drying over Europe. *Clim. Dyn., 27,* 281-299. doi:10.1007/s00382-006-0125-9

Schär, C., P.L. Vidale, D. Lüthi,C. Frei, C. Häberli, M.A. Liniger and C. Appenzeller (2004), The role of increasing temperature variability in European summer heat waves. *Nature, 427,* 332-336.

Seager, R., M. Ting, I. Held, Y. Kushnir, J. Lu, G. Vecchi, H.-P. Huang, N. Harnik, A. Leetma, N.-G. Lau, C. Li, J. Velez and N. Naik (2007), Model projections of an imminent transition to a more arid climate in southwestern North America. *Science, 316,* 1181-1184.

Sterl, A., C. Severijns, H. Dijkstra, W. Hazeleger, G.J. van Oldenborgh, M. van den Broeke, G. Burgers, B. van den Hurk, P.J. van Leeuwen and P. van Velthoven (2008), When can we expect extremely high surface temperatures? *Geophys. Res. Lett.* 35, L14703, doi:10.1029/2008GL034071.

Stott, P.A., D.A. Stone and M.R. Allen (2004), Human contribution to the European heat wave of 2003. *Nature, 432,* 610-614.

Ulden, A.P. van and G.J. van Oldenborgh (2006), Large-scale atmospheric circulation biases and changes in global climate model simulations and their importance for climate change in Central Europe. *Atm. Chem. Phys., 6,* 863-881.

Van den Hurk, B.J.J.M, P. Viterbo, A.C.M. Beljaars and A.K. Betts (2000), Offline validation of the ERA40 surface scheme. *ECMWF technical memorandum 295,* 43 pp.

Vautard, R., P. Yiou, F. D'Andrea, N. de Noblet, N. Viovy, C.Cassou, J. Polcher, P.Ciais, M. Kageyama and Y. Fan (2007), Summertime European heat and drought waves induced by wintertime Mediterranean rainfall deficit. *Geophys. Res. Lett., 34,* L07711, doi:10.1029/2006GL028001.

Figure Captions

Fig. 1: Difference between 1971-2000 and 2071-2100 during JJA for ECMWF (left) and ESSENCE (right) of MSLP[hPa] (a,b), SAT [°C] (c,d), geopotential height [m] zonally averaged over 0°E-30°E (e,f), PDF of daily mean zonal wind [m s^{-1}] averaged over 0°E-20°E, 40°N-50°N [blue: 1971-2000, red: 2071-2100] (g,h). For SAT the global mean change has been subtracted.

Fig. 2: Upper panels: First lagged SVD pair of soil wetness (a) in June and MSLP (b) [hPa] in July-August using all 17 ensemble members of ESSENCE for 1951-2000. The amplitude of the soil wetness pattern and the subsequent figures corresponds to one standard deviation of its amplitude time series, the amplitude of the MSLP pattern corresponds to the pressure response to a one standard deviation change in the soil

wetness pattern. The explained squared covariance is 63%. The correlation between both amplitude time series is 0.4. Middle and lower panels: Regressions between the amplitude time series of the soil wetness SVD pattern of (a) in June and evaporation [mm day^{-1}] (c), SAT [°C] (d) and precipitation [mm day^{-1}] (e) in July-August and precipitation in January-May [mm day^{-1}] (f).

Fig. 3 abcd: As Fig. 1aceg, but now for the MEDFLUX experiment.

Fig. 4: Climate change between 2071-2100 and 1971-2000 in JJA as simulated by the ECMWF model: (a) surface latent heat flux [W m^{-2}], (b) soil wetness SW (See text for explanation), (c) precipitation [mm day^{-1}], (d) Omega at 500 [hPa s^{-1}] and (e) net surface solar radiation [W m^{-2}]. The precipitation change during March-May is shown in (f).

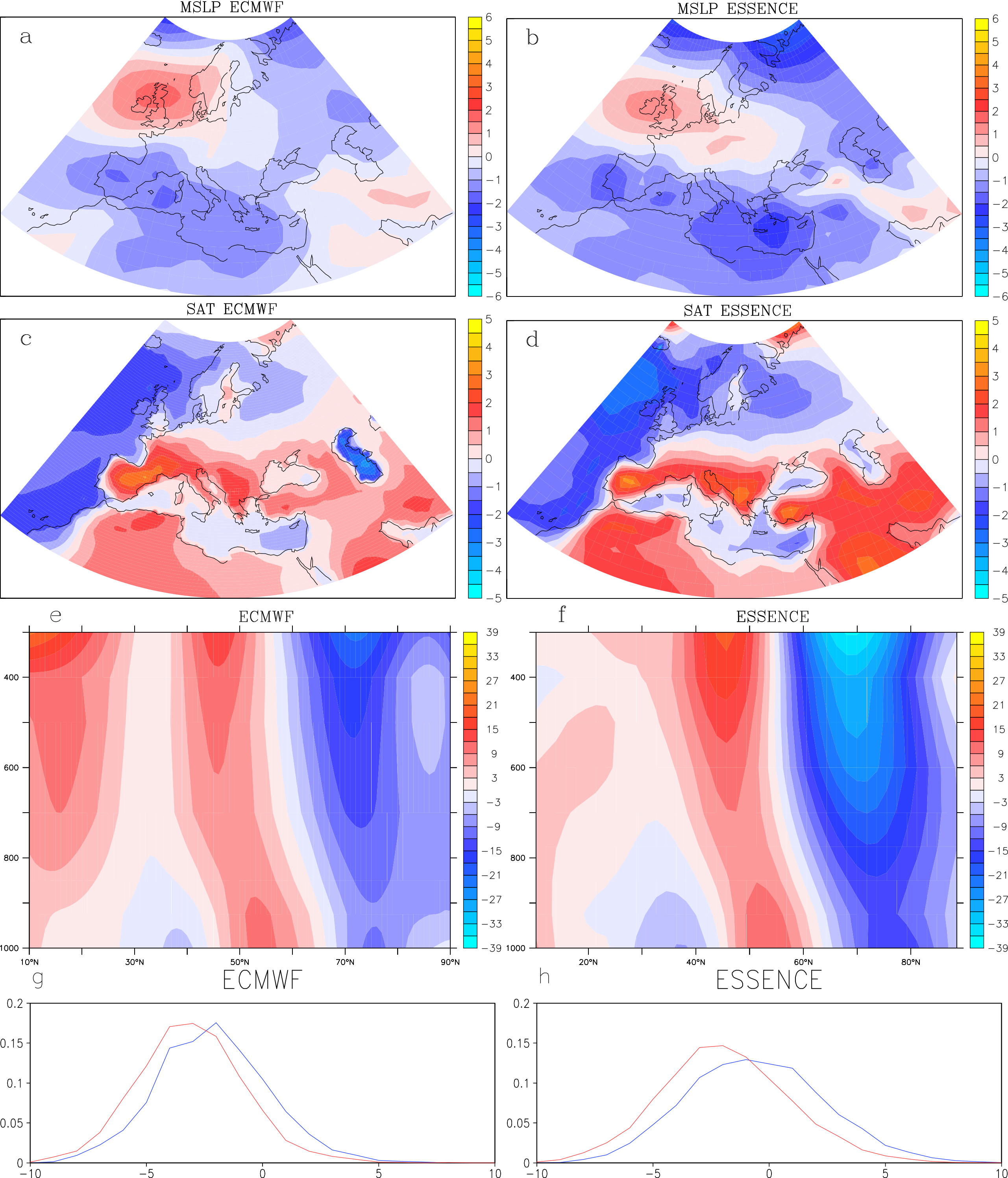

MSLP ECMWF
a
MSLP ESSENCE
b
6 5 4 3 2 1 0 −1 −2 −3 −4 −5 −6
SAT ECMWF
c
SAT ESSENCE
d
5 4 3 2 1 0 −1 −2 −3 −4 −5
e
ECMWF
f
ESSENCE
39 33 27 21 15 9 3 −3 −9 −15 −21 −27 −33 −39
400
600
800
1000
10°N 30°N 50°N 70°N 90°N
20°N 40°N 60°N 80°N
g
ECMWF
h
ESSENCE
0.2
0.15
0.1
0.05
0
−10 −5 0 5 10

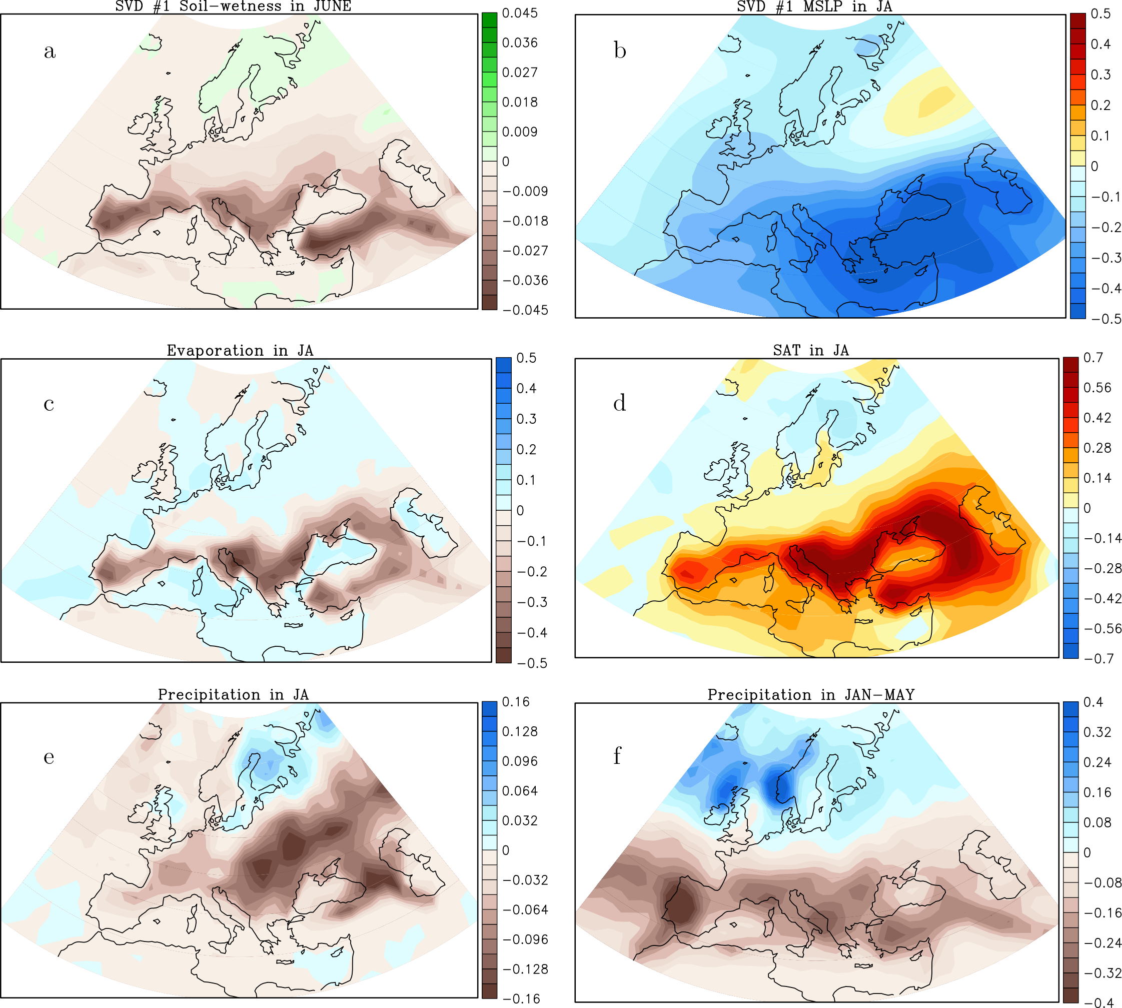

SVD #1 Soil-wetness in JUNE
a
0.045
0.036
0.027
0.018
0.009
0
−0.009
−0.018
−0.027
−0.036
−0.045
SVD #1 MSLP in JA
b
0.5
0.4
0.3
0.2
0.1
0
−0.1
−0.2
−0.3
−0.4
−0.5
Evaporation in JA
c
0.5
0.4
0.3
0.2
0.1
0
−0.1
−0.2
−0.3
−0.4
−0.5
SAT in JA
d
0.7
0.56
0.42
0.28
0.14
0
−0.14
−0.28
−0.42
−0.56
−0.7
Precipitation in JA
e
0.16
0.128
0.096
0.064
0.032
0
−0.032
−0.064
−0.096
−0.128
−0.16
Precipitation in JAN−MAY
f
0.4
0.32
0.24
0.16
0.08
0
−0.08
−0.16
−0.24
−0.32
−0.4

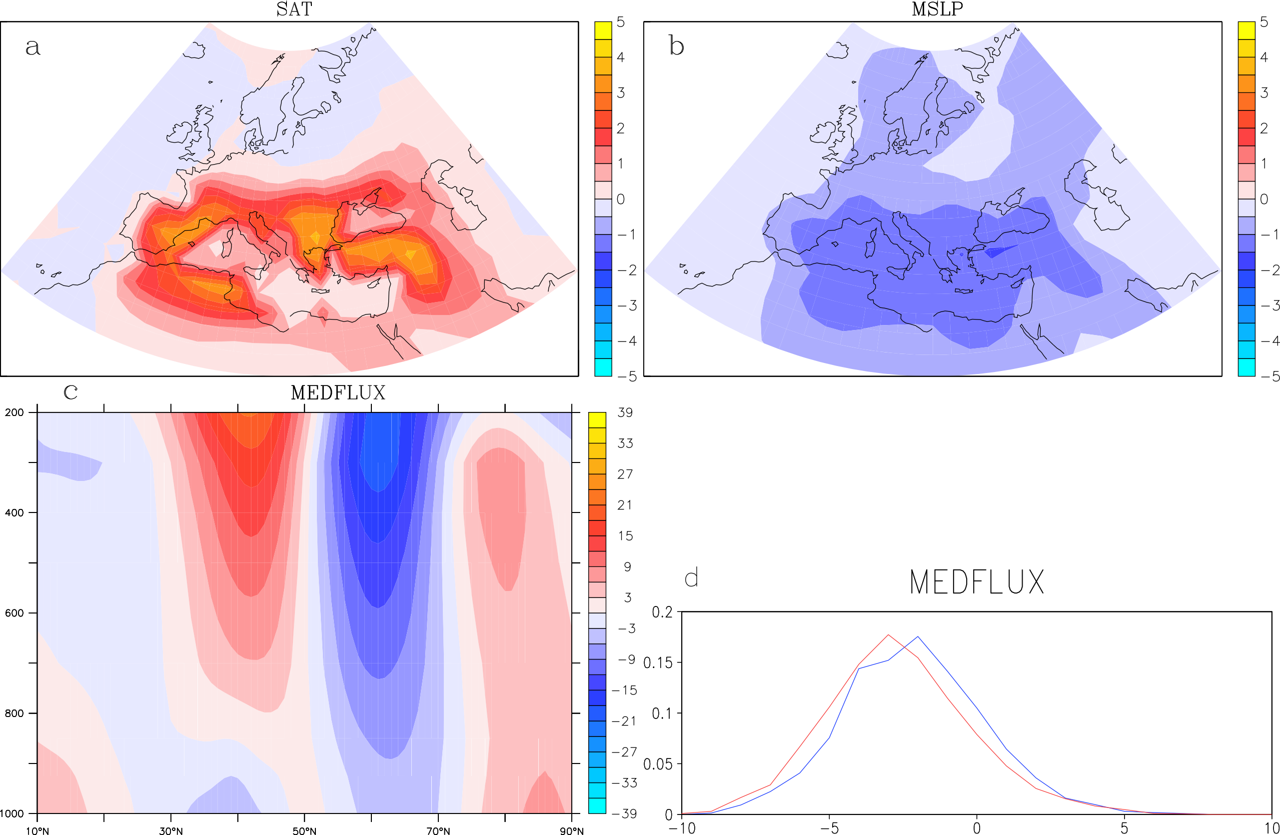

SAT
a
5
4
3
2
1
0
−1
−2
−3
−4
−5
MSLP
b
5
4
3
2
1
0
−1
−2
−3
−4
−5
c
MEDFLUX
200
400
600
800
1000
10°N
30°N
50°N
70°N
90°N
39
33
27
21
15
9
3
−3
−9
−15
−21
−27
−33
−39
d
MEDFLUX
0.2
0.15
0.1
0.05
0
−10
−5
0
5
10

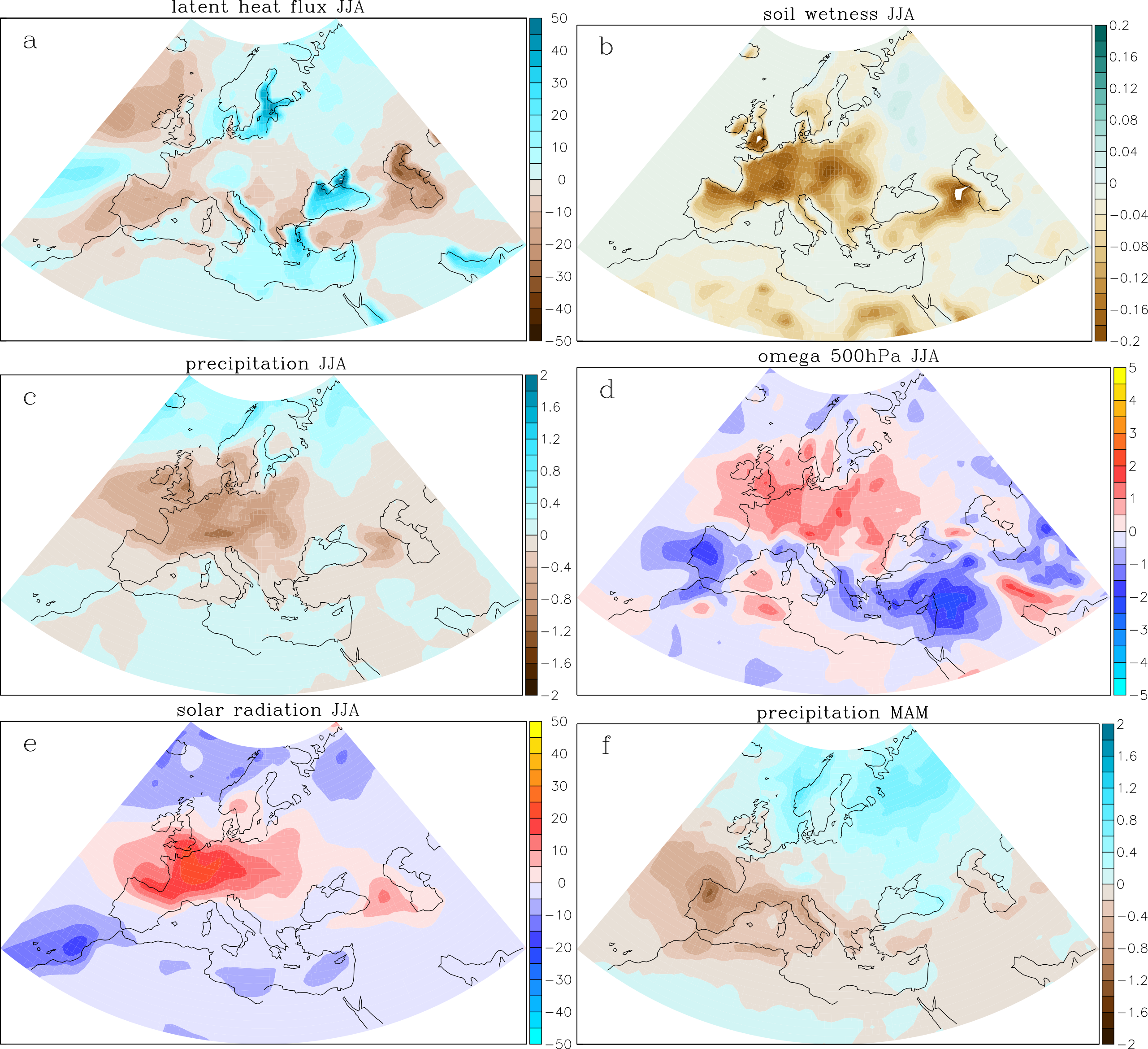

latent heat flux JJA
a
50
40
30
20
10
0
−10
−20
−30
−40
−50
soil wetness JJA
b
0.2
0.16
0.12
0.08
0.04
0
−0.04
−0.08
−0.12
−0.16
−0.2
precipitation JJA
c
2
1.6
1.2
0.8
0.4
0
−0.4
−0.8
−1.2
−1.6
−2
omega 500hPa JJA
d
5
4
3
2
1
0
−1
−2
−3
−4
−5
solar radiation JJA
e
50
40
30
20
10
0
−10
−20
−30
−40
−50
precipitation MAM
f
2
1.6
1.2
0.8
0.4
0
−0.4
−0.8
−1.2
−1.6
−2